

Measuring adhesion, attraction, and repulsion between surfaces in liquids with an atomic-force microscope

A. L. Weisenhorn*

Department of Physics, University of California, Santa Barbara, California 93106

P. Maivald

Digital Instruments, 6780 Cortona Drive, Santa Barbara, California 93117

H.-J. Butt

Max-Planck-Institut für Biophysik, Kennedyallee 70, D-6000 Frankfurt 70, Germany

P. K. Hansma

Department of Physics, University of California, Santa Barbara, California 93106

(Received 17 May 1991; revised manuscript received 15 January 1992)

Understanding the forces such as adhesion, attraction, and repulsion between surfaces and liquids is the key not only to understanding phenomena such as lubrication and indentation but also the key to understanding how best to operate an atomic-force microscope (AFM). In this paper, we examined the cases of an insulating tip on an insulating sample (silicon nitride tip on mica) and of a conducting tip on a conducting sample (tungsten carbide tip on a gold or platinum foil). The force-versus-distance curves for these two limiting systems were very different in different liquids. In ethanol, the curve is just what one would expect theoretically: a slightly attractive force before contact, a jump into contact, then a small pull-out force, about 0.2 nN for an insulating tip on the insulating surface and about 0.5 nN for two conducting surfaces. In pure water, the behavior is complex and variable. Pull-out forces vary from 0.2 to 1.5 nN for two insulating surfaces. For two conducting surfaces the force-versus-distance curves show large pull-out forces of order of 10 nN. These large forces are probably due to adsorption contamination layers on the metal surfaces that are not removed by the solvent action of the pure water. These forces, however, can be reduced to less than one-hundredth of the original value by adding ethanol to the water. This makes ethanol a useful liquid for routine imaging of macromolecules such as DNA, proteins, and polymers, that have been adsorbed to a substrate and that must be imaged at low force. In formamide, we observed a predicted repulsive interaction in the nontouching regime for insulating surfaces as predicted by Hartmann. In different concentrations of KCl aqueous solution, we observed again a repulsive interaction in the nontouching regime due to double-layer repulsion of charged surfaces across ionic solutions. The measured Debye length agrees well with the theoretical prediction. And last, the dependence of the pull-out force on the indentation in water has been investigated. The more the tip indents the sample surface in a force-versus-distance cycle, the larger the pull-out force will be. This shows also the usefulness of the AFM for investigations of micromechanical properties.

INTRODUCTION

The atomic-force microscope (AFM) (Refs. 1 and 2) has proved its usefulness in imaging surfaces with atomic or molecular resolution in air,³⁻⁷ vacuum,⁸ or liquids⁹⁻¹² when scanning in the contact mode. The underlying contrast mechanism and the limitation of the AFM in both the resolution and the nondestructive scanning¹³ are based on the interaction between the sample surface and the AFM tip. Earlier experimental works have shown that scanning in air always involves large meniscus forces of the order of 100 nN.¹⁴⁻¹⁹ In other experiments monolayer films^{20,21} and transition-metal dichalcogenides²² were probed with AFM's. Using a metal tip on a metal surface gives rise to metallic adhesion of the order of a few nN,^{23,24} which was confirmed by calculation,²⁵ or of a few μN ;²⁶ other theoretical calculations give forces of the order of 10 nN.^{26,27} Furthermore, it was suggested that

the force for nondestructive scanning should not exceed 1–10 nN for “hard” surfaces²⁷⁻²⁹ and 10 pN for soft surfaces such as biological surfaces.³⁰ In order to overcome the huge meniscus force, scanning in UHV or under liquids is required. We report here the interaction between an AFM tip and a sample surface in ethanol, water, formamide, and KCl aqueous solution by studying force-versus-distance curves.

EXPERIMENT

A commercial AFM (the Nanoscope II Force Microscope³¹) including electronic control and software was used to record the force-versus-distance curves, revealing the interaction between the surface of the sample and the tip. A force-versus-distance curve (see Fig. 1) displays the deflection of the cantilever (the y axis of the force-versus-distance curve), on which the tip is mounted as a

function of the vertical position of the xyz translator (the x axis of the force-versus-distance curve) on which the sample is mounted (for schematic details of an AFM see Ref. 7). The xyz translator moves the sample surface up and down with a constant speed (except at the turning points). The total time t_c for a complete up and down cycle was chosen long enough that there was no hysteresis in the *nontouching regime*, i.e., where the tip is not touching the sample surface. All the force-versus-distance curves displayed a *single* measurement while the xyz translator was continuously going through the up and down cycle. A liquid cell makes it possible to immerse both the tip and the sample surface completely in a

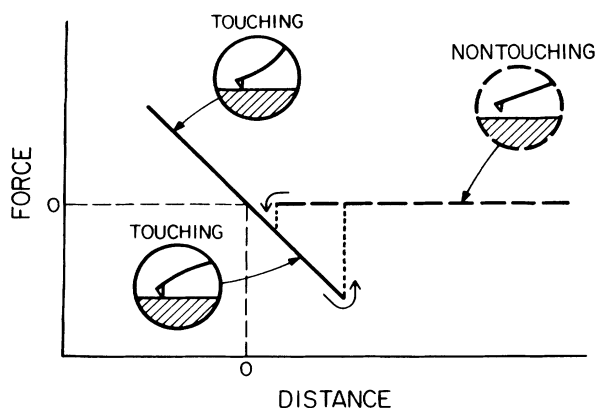


FIG. 1. Diagram of a typical force-vs-distance curve. The x axis represents the distance by which the xyz translator and hence the sample surface moves up and down. The sample surface approaches the tip when going to the left in the force-vs-distance curve. The y axis represents the signal of the two-segment photodiode, which is proportional to the deflection of the cantilever and therefore the force of the cantilever spring (for more details see Ref. 7). Deflecting the cantilever away from the sample surface is going upwards in the force-vs-distance curve. Following a whole cycle in the force-vs-distance curve, we start at a large tip-sample separation in the *nontouching regime* (the right edge of the force-vs-distance curve). From there, without or with only little deflection of the cantilever, the sample approaches the tip following along the horizontal (*nontouching*) line to the left in the force-vs-distance curve. At a certain point (the jump-in point in the force-vs-distance curve) the transition from nontouching to touching occurs, i.e., the tip “jumps onto” the sample surface. This transition can be very complex, especially when high forces occur and adsorbed layers are involved. Moving the sample still further causes deflection of the cantilever for the same amount the sample is moved (the *touching regime*); this is represented by the diagonal (*touching*) line in the left part of the force-vs-distance curve. Retracting then the sample from the tip, i.e., going to the right in the force-vs-distance curve, the cantilever moves first again with the sample. It can even deflect towards the sample before the tip breaks the contact to the sample surface, going through the *point of minimal force* in the force-vs-distance curve. We define the difference between this minimal force and the nontouching line as the pull-out force. At the jump-out point, the transition from touching to nontouching, the tip has completely lost contact with the surface or the adsorbed layers on the surface; the force-vs-distance curve returns to the nontouching line.

liquid. Freshly cleaved mica,³² flame polished^{33,34} gold foil³⁵ or platinum foil³⁶ were used as sample surface. The tip was a microfabricated Si_3N_4 tip³⁷⁻³⁹ (estimated tip radius: ≈ 50 nm) or a shard of tungsten carbide (WC), that was glued on a cantilever with two-ton clear epoxy.⁴⁰ The WC shards were obtained by putting a piece of WC between two hardened, flat steel plates and hammering on the top one. Therefore, the tip radius is difficult to determine. Ethanol (99.8%),⁴¹ deionized water (resistivity: 16 $\text{M}\Omega$),⁴² formamide (methanamide, CH_3NO),⁴³ and different concentrations of KCl aqueous solution were introduced in the liquid cell after the sample was mounted on the xyz translator of the AFM, and the cantilever with microfabricated tip was put in place.

RESULTS AND DISCUSSION

The force-versus-distance curves reveal the forces of the AFM tip interacting with a sample surface across a third medium—in this report, liquids (for a good description of two media interacting across a third medium see Refs. 44 and 45). Figure 2(a) shows a force-versus-distance curve using ethanol between a Si_3N_4 tip and a mica surface. The pull-out force is about 0.2 nN. Even in the case of metal-metal interaction (WC tip on gold) the pull-out force is only about 0.5 nN [Fig. 2(b)]. For metal-nonmetal interaction (Si_3N_4 tip on gold or WC tip on mica) the pull-out force is between 0.2 and 0.5 nN. It is important to note that the amount of hysteresis also depends on the spring constant of the cantilever. For exactly the same tip-liquid-sample system a significantly (i.e., roughly one order of magnitude) softer cantilever would show larger hysteresis in force units. Thus detailed numerical comparisons can only be made with cantilevers of the same spring constant. This does not, however, change our qualitative conclusions, since whenever an increase in hysteresis was observed we were using the same or even a stiffer cantilever.

The small attractive force just before the tip jumps into contact is due to van der Waals interaction. The small pull-out force for ethanol makes it possible to use it for imaging very delicate surfaces such as DNA (Ref. 46) with forces < 0.1 nN. (Note that the imaging force is measured from the point of minimal force in the force-versus-distance curve to the operating point. The end atoms of the tip and the top atoms of the sample surface that are in contact with the tip always repel each other. Reducing this repulsion by lowering the operating point and the size of the hysteresis guarantees the best imaging of soft samples with the AFM.)

When water is used instead of ethanol for Si_3N_4 tip on mica, the pull-out force is larger and varies from 0.2 to 1.5 nN [Figs. 3(a) and 3(b)]. This is in good agreement with earlier results taken with an older AFM.¹⁶ Here, the small force prior to the jump into contact is repulsive. This is due to double-layer repulsion (see the more detailed discussion of Figs. 6 and 7). In the case of metal-nonmetal interaction (the Si_3N_4 tip on gold or the WC tip on mica) the pull-out force is between 0.5 and 2.0 nN. For a WC tip on a gold surface in water the pull-out force goes up to about 10 nN [Fig. 3(c)]. Furthermore

the *pull-in* and *pull-out* distances, which are measured from the pull-in and pull-out points, respectively, on the nontouching line to the intersection of the extended nontouching line with the touching line are 22 and 37 nm, respectively. The transition from nontouching to touching and vice versa is much more complex than in Figs. 3(a) and 3(b); it goes through at least two instances of “jump-in” and “jump-out.” This is due to the meniscus forces of the layers of organic molecules (see chapter 14.4 in Ref.

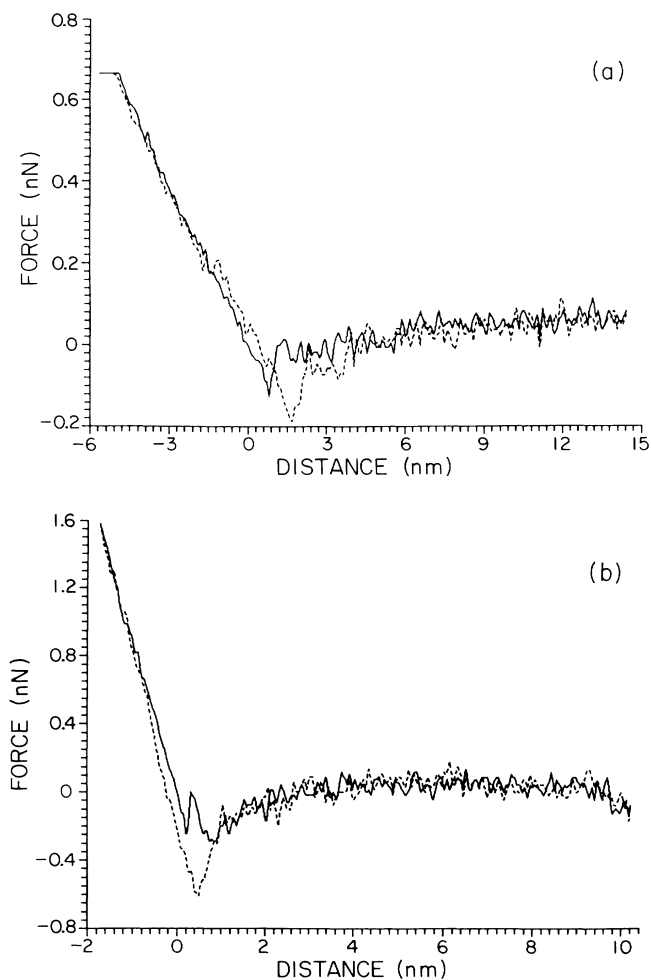


FIG. 2. Force-vs-distance curves in ethanol. The solid line shows the motion of the sample towards the tip, the dashed line from the tip. The units of the y axis are calculated by multiplying the units of the x axis with the spring constant k and then dividing the product by the slope s of the solid touching line in the left part of the force-vs-distance curve. It will be indicated when the dashed touching line was used to determine the slope. In the touching regime the tip is in contact with the sample surface and is deflecting for the same distance the sample is moving up or down. The origin of the force-vs-distance curve is chosen at the intersection of the extended nontouching line and the touching line. t_c is the time for a complete up and down cycle. (a) Si_3N_4 tip ($k=0.13$ N/m) on mica ($t_c=0.1$ ms). The horizontal line at the left edge is due to saturation of the signal processor. (b) WC tip ($k=0.9$ N/m) on gold ($t_c=2000$ ms). The attractive force in (a) and (b) just before the tip jumps into contact is due to van der Waals interaction.

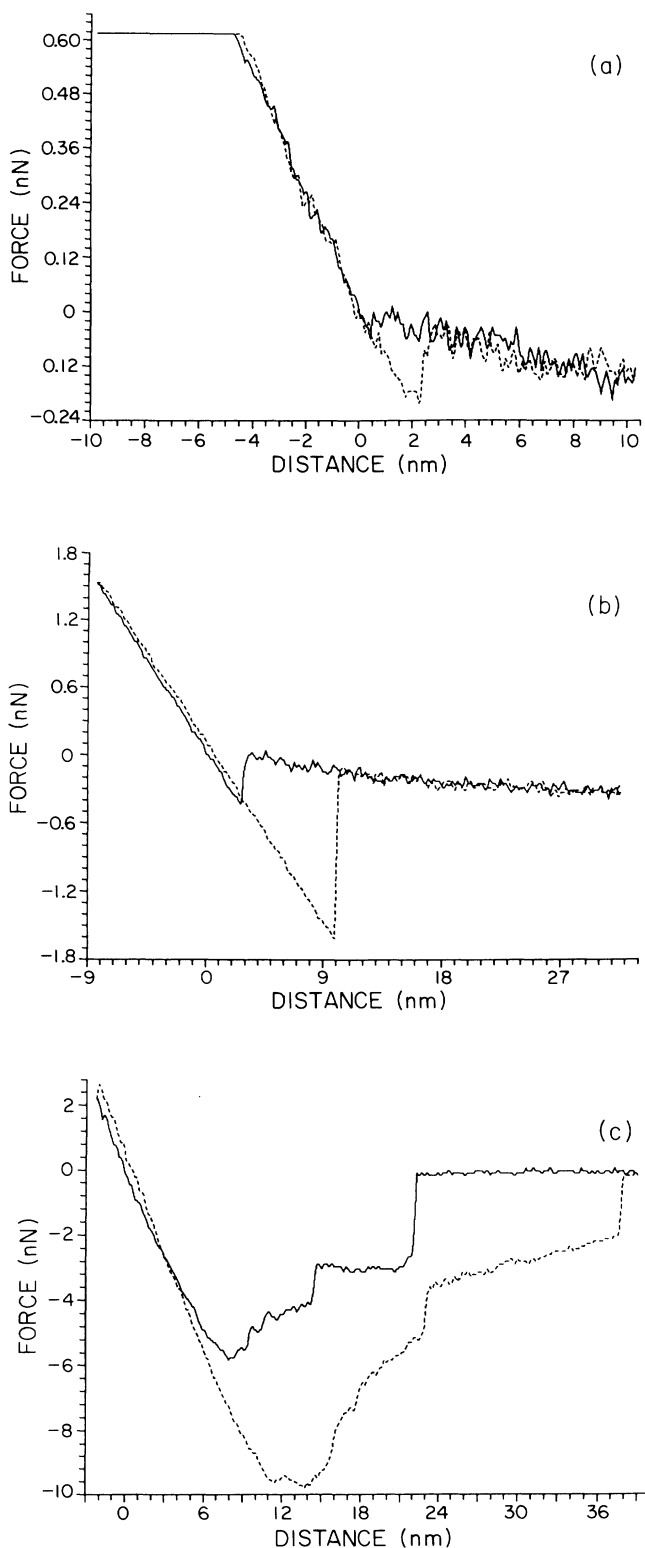


FIG. 3. Force-vs-distance curves in water. (a) Si_3N_4 tip ($k=0.13$ N/m) on mica ($t_c=0.5$ ms). Again the horizontal line at the left edge indicates saturation of the signal processor. (b) Si_3N_4 tip ($k=0.18$ N/m) on mica ($t_c=400$ ms). Note the variation in (a) and (b) due to different tips and the repulsive interaction in the nontouching regime. (c) WC tip ($k=0.9$ N/m) on gold ($t_c=80$ ms).

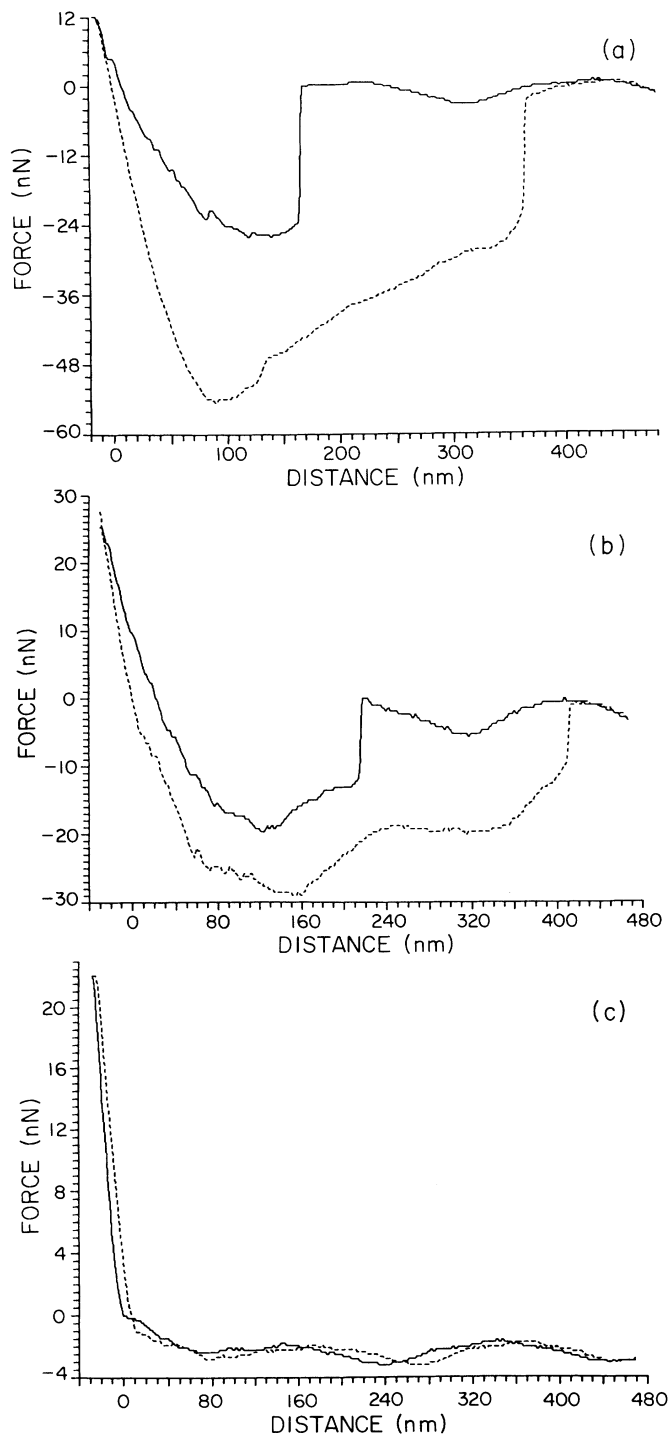


FIG. 4. Force-vs-distance curves of the WC tip ($k=0.9$ N/m) on platinum ($t_c=520$ ms): (a) in water (slope: dashed touching line; note that the units of the y axis are not very accurate because the slope could not be determined very precisely), (b) after adding ethanol (the estimated volume is less than $\frac{1}{4}$ of the liquid cell; slope: dashed touching line), (c) after flushing the liquid cell thoroughly with ethanol (slope: solid touching line). The oscillation of the nontouching line ($\lambda_0 \approx 200$ nm $\pm 20\%$) is caused by interference of the laser beam ($\lambda_{\text{laser}}=670$ nm $\approx 2n_{\text{ethanol}}\lambda_0$, $n_{\text{ethanol}}=1.362$) that is reflected on the gold foil with the one that is reflected on the cantilever. This oscillation was never observed, when mica was used.

44), which make an originally hydrophilic gold surface hydrophobic within a few seconds when it is exposed to air due to the adsorption of organic molecules.⁴⁷ Such layers caused a similar transition with an even larger pull-out force when the experiment was done in air.¹⁶ These layers can be removed and hence the pull-out force can be drastically reduced when ethanol is used.

The effect of removing these layers was directly observed in the next experiment, where water was originally between the WC tip and a platinum surface [Fig. 4(a)]. The force-versus-distance curve showed a large hysteresis (pull-in and pull-out forces are about 26 and 55 nN, respectively). The hysteresis was then reduced continuously to less than one-hundredth of the original value by adding more and more ethanol [Figs. 4(b) and 4(c)] while the cycles through the force-versus-distance curve were not disrupted; the pull-in and pull-out forces in Fig. 4(b) are about 20 and 29 nN, respectively. We have observed the same kinds of hysteresis when we started with pure ethanol and then added water.

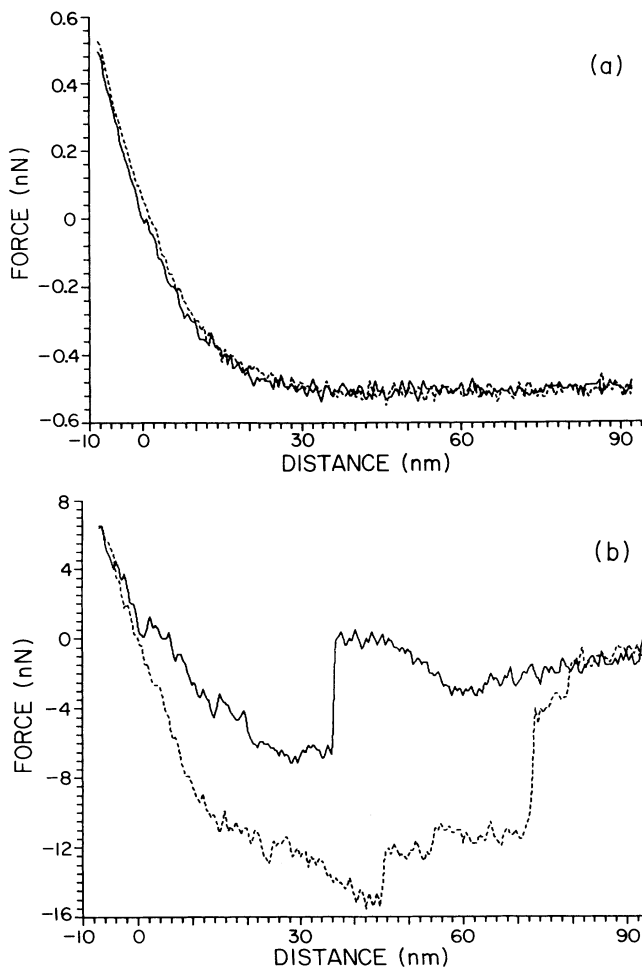


FIG. 5. Force-vs-distance curves in formamide: (a) Si_3N_4 tip ($k=0.06$ N/m) on mica ($t_c=1000$ ms; slope: solid touching line). Note the repulsive interaction in the nontouching regime. (b) WC tip ($k=0.9$ N/m) on gold ($t_c=80$ ms; slope: dashed touching line). Again the oscillation of the nontouching line is caused by interference.

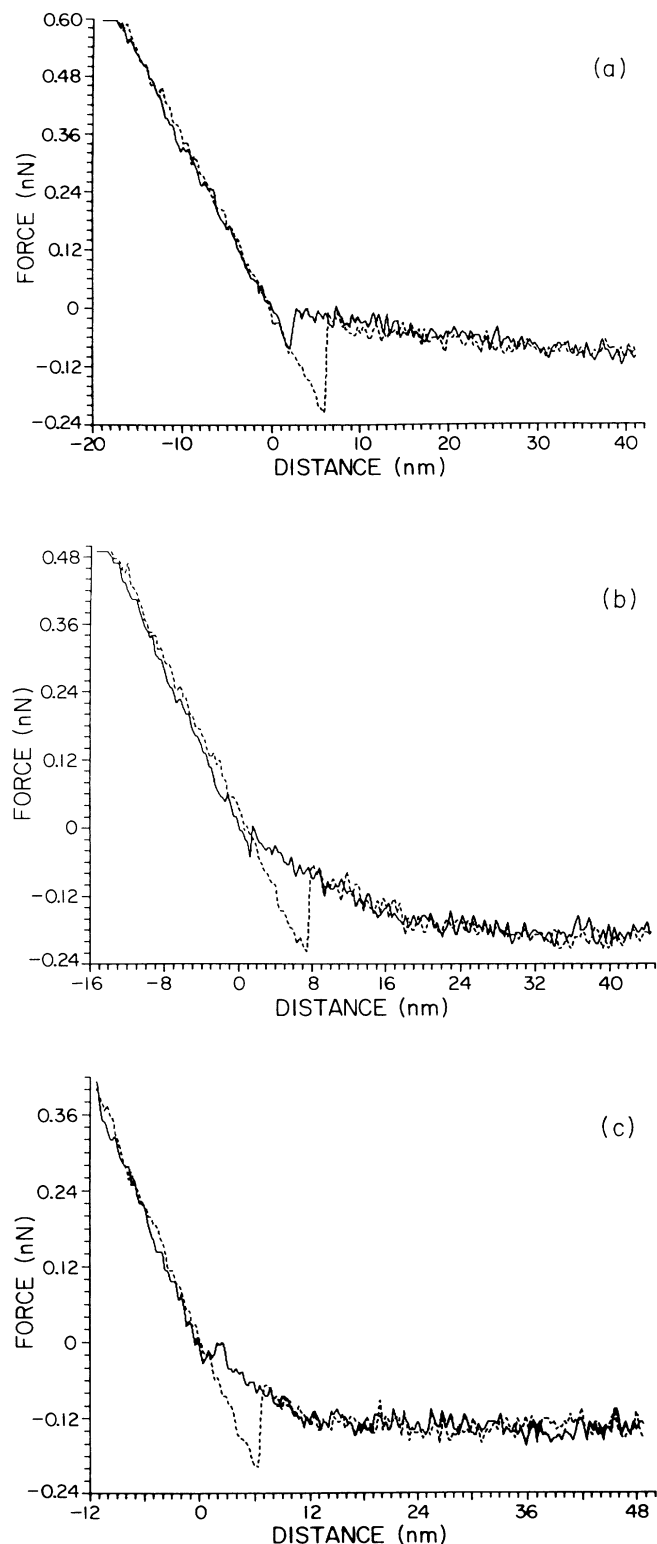


FIG. 6. Force-vs-distance curves of the Si_3N_4 tip ($k=0.035$ N/m) on mica in KCl aqueous solution, $\text{pH} \approx 6.6$ ($t_c=2300$ ms). The KCl concentrations are (a) 0.1 mM, (b) 1 mM, and (c) 10 mM. The force curves show repulsive behavior in the nontouching regime. For two equally charged and flat surfaces the repulsion is decaying exponentially with increasing distance x ($\sim e^{-\kappa x}$, where $1/\kappa$ is defined as Debye length).

Figure 5(a) shows the force-versus-distance curve of a Si_3N_4 tip on mica in formamide. The repulsive behavior in the nontouching regime can clearly be seen between the nontouching line and the touching line in the left of the force-versus-distance curve. This effect is due to dominant entropic contribution to the interaction as described by Hartmann.⁴⁸ For metal-nonmetal interaction (the Si_3N_4 tip on gold or the WC tip on mica) no repulsive behavior in the nontouching regime was found. In the case of metal-metal (the WC tip on gold) interaction in formamide [Fig. 5(b)] the force-versus-distance curve looks similar to the one in water. The pull-out force is about 15 nN, and the pull-in and pull-out distances are 37 and 80 nm, respectively. Another WC tip and platinum foil instead of gold foil gave similar force-versus-distance curves for Figs. 2(b), 3(c), and 5(b). The difference in the amount of the hysteresis in the case of metal-metal interaction in different liquids [Figs. 3(c), 4(a)–4(c), and 5(b)] is caused by different degrees of hydrophobicity and attractivity of the surface to adsorb organic molecules and by different solubilities of these molecules in the present liquid.

Imaging biological samples in their natural environment means imaging them in salty solutions such as a KCl aqueous solution. Figures 6(a)–6(c) show force-versus-distance curves of a Si_3N_4 tip on mica in (a) 0.1, (b) 1, and (c) 10 mM-KCl aqueous solution, using an even softer cantilever than for the previous figures. While the

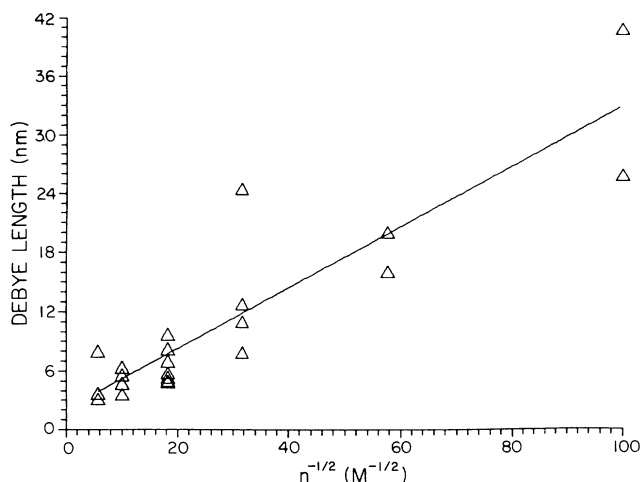


FIG. 7. Each point represents one force-vs-distance curve and gives the Debye length $1/\kappa$ for a specific KCl concentration; the Debye length-vs-inverse square root of the concentration $1/\sqrt{n}$ is plotted for concentrations from 0.1 to 30 mM. The Debye length $1/\kappa$ was determined from the upper (approaching) force-vs-distance curves by least-square fits of the repulsive, nontouching regime with the function $y - C = Ae^{-Bx}$. Actually linear regression was calculated for $\ln(y - C) = \ln A - Bx$, where C served as a parameter and was chosen in such a way that it minimized the least-square error. Only points whose linear regression correlation coefficient $|r| > 0.8$ were used in this plot (Ref. 52). The linear regression of all the used points is $1/\kappa$ (nm) = $0.3 \pm 0.1n^{-0.5}$ ($\text{M}^{-0.5}$) + 3 ± 2 .

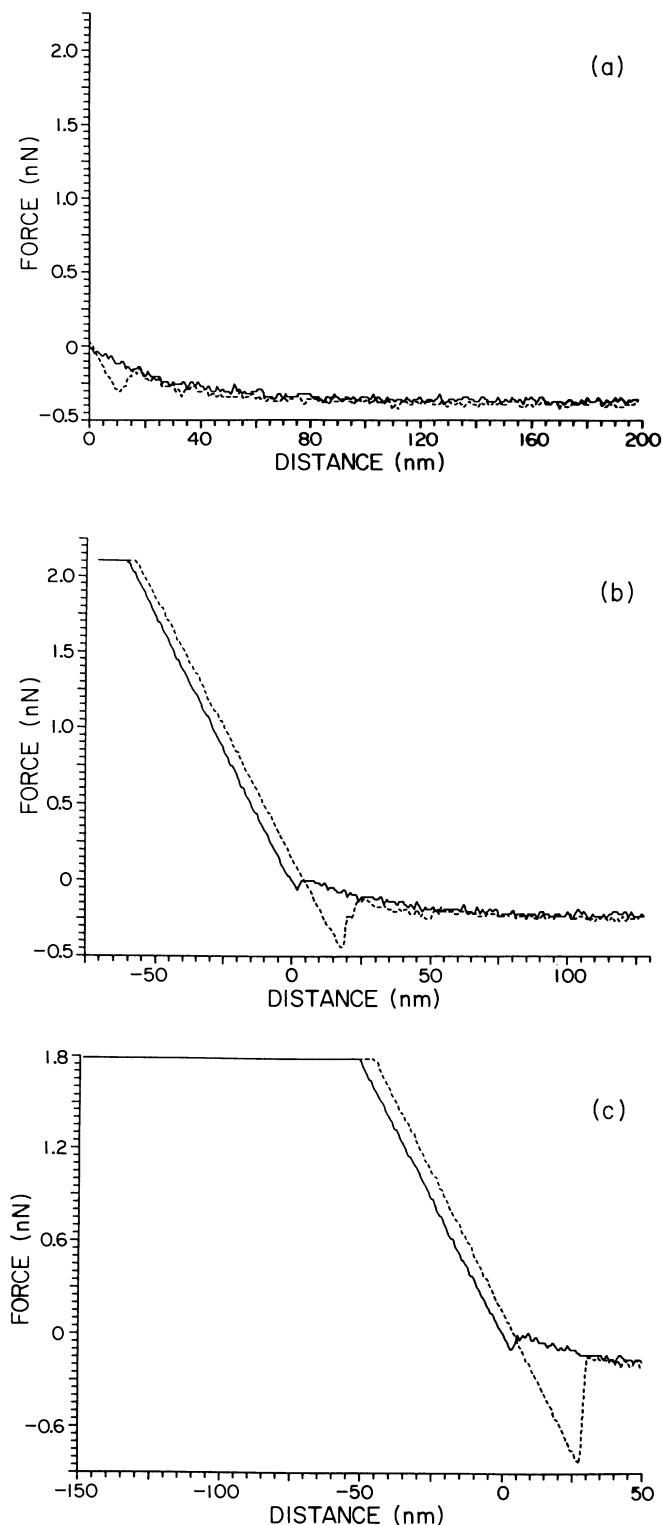


FIG. 8. Force-vs-distance curves of the Si_3N_4 tip ($k=0.035$ N/m) on mica in water ($t_c=200$ ms). Note again the repulsive behavior in the nontouching regime due to double-layer repulsion. The pull-out force increases with increased indentation. The indentation is measured from the origin to the left edge of the force-vs-distance curve; again the horizontal curve at the left is due to saturation. The indentation is (a) < 10 nm (< 0.35 nN), (b) 70 nm (2.5 nN), and (c) 150 nm (5.3 nN).

sample surface approaches the tip, repulsive interaction occurs in the nontouching regime. (Note that the AFM can directly measure the interaction between tip and sample in the nontouching regime and the deformation of the sample in the touching regime.) The pull-out forces are (a) 0.2 , (b) 0.15 , and (c) 0.2 nN. With increasing KCl concentration the repulsion rises more over the same distance. This repulsion is due to double-layer forces of charged surfaces in an ionic solution (see, for example, chapter 12 of Ref. 44). For two equally charged flat surfaces the repulsion decays exponentially $\sim e^{-\kappa x}$, where x is the distance between the surfaces. For low surface potentials (25 mV)

$$\kappa = \left[\frac{ne^2}{\epsilon\epsilon_0 kT} \right]^{1/2} \quad \text{or} \quad \frac{1}{\kappa} = 0.305 \text{ nm} \times \sqrt{1 \text{ M}/n},$$

where n is the ionic concentration, $\epsilon=79$, and $T=297$ K. The characteristic length $1/\kappa$ is called the Debye length. In Fig. 7 the Debye length was plotted versus the inverse square root of the KCl concentration. The linear regression of all the plotted data points gives a slope of 0.308 . This is in good agreement with the theoretical value of 0.305 , considering that we use in our setup a flat surface and a spherical surface of different materials (instead of two flat surfaces of the same material).⁴⁹ Furthermore, there is also an uncertainty in the z calibration of the xyz translator and in the accuracy of the KCl concentration.

In the last experiment the influence of indentation on the pull-out force was investigated. In Fig. 8(a) the pull-out force was about 0.2 nN for < 10 nm indentation, which corresponds to an indentation force of < 0.35 nN. Increasing the indentation to 70 nm (2.5 nN) in Fig. 8(b) and 150 nm (5.3 nN) in Fig. 8(c) results in increased pull-out forces of 0.35 and 0.7 nN, respectively. This agrees well with the observation made with a surface-force apparatus.⁵⁰ The adhesion between most of the surfaces increases when the indentation is increased.⁵¹

We have shown that the AFM is a useful tool to measure adhesion, attraction, and repulsion between conducting and nonconducting sample surfaces and tips across a liquid medium. The AFM can also be used to measure directly the attractive and repulsive interaction and determine, for example, the Debye length of double-layer repulsion. Furthermore, the AFM can reveal mechanical properties in experiments where indentation is involved.

ACKNOWLEDGMENTS

We would like to thank J.N. Israelachvili, C.A. Helm, D. Leckband, U. Hartmann, F. Lange, and B. Velamakanni for helpful discussions, G.L. Kelderman, S.A.C. Gould, J. Cleveland, K. Kjoller, and E. Martzen for technical support, and J. Gurley and V. Elings for software support. This research was also supported in part by IBM (A.L.W.), by MPI (H.-J.B.), by the Deutsche Forschungsgemeinschaft SFB 169 (H.-J.B.), and by a National Science Foundation-Solid State Physics Grant No. DMR89-17164 (P.K.H.).

- *Permanent address: Institute of Histology, University P erolles, CH-1700 Fribourg, Switzerland; FAX: +41 37 826 527.
- ¹G. Binnig, C. F. Quate, and Ch. Gerber, *Phys. Rev. Lett.* **56**, 930 (1986).
 - ²D. Rugar and P. K. Hansma, *Physics Today* **43**(10), 23 (1990).
 - ³G. Binnig, Ch. Gerber, E. Stoll, T. R. Albrecht, and C. F. Quate, *Europhys. Lett.* **3**, 1281 (1987).
 - ⁴T. R. Albrecht and C.F. Quate, *J. Appl. Phys.* **62**, 2599 (1987).
 - ⁵O. Marti, B. Drake, S. A. C. Gould, and P. K. Hansma, *J. Vac. Sci. Technol. A* **6**, 287 (1988).
 - ⁶P. K. Hansma, V. B. Elings, O. Marti, and C. E. Bracker, *Science* **242**, 209 (1988).
 - ⁷S. A. C. Gould, B. Drake, C. B. Prater, A. L. Weisenhorn, S. Manne, G. L. Kelderman, H.-J. Butt, H. G. Hansma, P. K. Hansma, S. Magonov, and H.-J. Cantow, *Ultramicroscopy* **33**, 93 (1990).
 - ⁸G. Meyer and N. M. Amer, *Appl. Phys. Lett.* **53**, 2400 (1988).
 - ⁹B. Drake, C. B. Prater, A. L. Weisenhorn, S. A. C. Gould, T. R. Albrecht, C. F. Quate, D. S. Cannell, H. G. Hansma, and P. K. Hansma, *Science* **243**, 1586 (1989).
 - ¹⁰A. L. Weisenhorn, J. E. MacDougall, S. A. C. Gould, S. D. Cox, W. S. Wise, J. Massie, P. Maivald, V. B. Elings, G. D. Stucky, and P. K. Hansma, *Science* **247**, 1330 (1990).
 - ¹¹S. Manne, H. J. Butt, S. A. C. Gould, and P. K. Hansma, *Appl. Phys. Lett.* **56**, 1758 (1990).
 - ¹²A. L. Weisenhorn, M. Egger, F. Ohnesorge, S. A. C. Gould, S.-P. Heyn, H. G. Hansma, R. L. Sinsheimer, H. E. Gaub, and P. K. Hansma, *Langmuir* **7**, 8 (1991).
 - ¹³J. B. Pethica and W. C. Oliver, *Phys. Scr. T* **19**, 61 (1987).
 - ¹⁴Y. Martin, C. C. Williams, and H. K. Wickramasinghe, *Scanning Microsc.* **2**, 3 (1988).
 - ¹⁵E. Meyer, H. Heinzlmann, P. Gr tter, Th. Jung, T. Weisskopf, H.-R. Hidber, R. Lapka, H. Rudin, and H.-J. G ntherodt, *J. Microsc.* **152**, 269 (1988).
 - ¹⁶A. L. Weisenhorn, P. K. Hansma, T. R. Albrecht, and C. F. Quate, *Appl. Phys. Lett.* **54**, 2651 (1989).
 - ¹⁷N. A. Burnham and R. J. Colton, *J. Vac. Sci. Technol. A* **7**, 2906 (1989).
 - ¹⁸C. M. Mate, M. R. Lorenz, and V. J. Novotny, *J. Chem. Phys.* **90**, 7550 (1989).
 - ¹⁹W. A. Ducker, R. F. Cook, and D. R. Clarke, *J. Appl. Phys.* **67**, 4045 (1990).
 - ²⁰N. A. Burnham, D. D. Dominguez, R. L. Mowey, and R. J. Colton, *Phys. Rev. Lett.* **64**, 1931 (1990).
 - ²¹G. S. Blackman, C. M. Mate, and M. R. Philpott, *Phys. Rev. Lett.* **65**, 2270 (1990).
 - ²²E. Meyer, D. Anselmetti, R. Wiesendanger, H.-J. G ntherodt, F. L vy, and H. Berger, *Europhys. Lett.* **9**, 695 (1989).
 - ²³U. D rig, O. Z ger, and D. W. Pohl, *J. Microsc.* **152**, 259 (1988).
 - ²⁴U. D rig, O. Z ger, and D. W. Pohl, *Phys. Rev. Lett.* **65**, 349 (1990).
 - ²⁵C. Julian Chen, *J. Phys. Condens. Matter* **3**, 1227 (1991).
 - ²⁶U. Landman, W. D. Luedtke, N. A. Burnham, and R. J. Colton, *Science* **248**, 454 (1990).
 - ²⁷F. O. Goodman and N. Garcia, *Phys. Rev. B* **43**, 4728 (1991).
 - ²⁸F. F. Abraham, I. P. Batra, and S. Ciraci, *Phys. Rev. Lett.* **60**, 1314 (1988).
 - ²⁹F. F. Abraham and I. P. Batra, *Surf. Sci.* **209**, L125 (1989).
 - ³⁰B. N. J. Persson, *Chem. Phys. Lett.* **141**, 366 (1987).
 - ³¹Digital Instruments, Inc., 6780 Cortona Drive, Santa Barbara, CA 93117.
 - ³²Muscovite mica from Asheville-Schoemaker, P. O. Box 318, Newport News, VA.
 - ³³J. Clavilier, R. Faure, G. Guinet, and R. Durand, *J. Electroanal. Chem.* **107**, 205 (1980).
 - ³⁴J. Wiechers, T. Twomey, D. M. Kolb, and R. J. Behm, *J. Electroanal. Chem.* **248**, 451 (1988).
 - ³⁵Johnson Matthey Electronics, Ward Hill, MA 01835.
 - ³⁶Alfa Products, Danvers, MA 01923.
 - ³⁷Since the Si₃N₄ tips were made by vapor-deposition technique, the exact [Si]:[N] ratio is not determined. The range is Si₃₋₁₅N₄. Personal communication by Shinya Akamine.
 - ³⁸Thomas R. Albrecht, dissertation, Stanford University, 1989.
 - ³⁹T. R. Albrecht, S. Akamine, T. E. Carver, and C. F. Quate, *J. Vac. Sci. Technol. A* **8**, 3386 (1990).
 - ⁴⁰Devcon Corporation, Danvers, MA 01923.
 - ⁴¹Balzers Union, CH-9470 Buchs, Switzerland.
 - ⁴²Milli-Q, water purification system by Millipor Corporation, Bedford, MA 01730.
 - ⁴³From Sigma Chemical Co., St. Louis, MO.
 - ⁴⁴J. N. Israelachvili, *Intermolecular and Surface Forces with Applications to Colloidal and Biological Systems* (Academic, New York, 1985).
 - ⁴⁵H.-J. Butt, *Biophys. J.* **60**, 777 (1991); **60**, 1438 (1991).
 - ⁴⁶H. G. Hansma, A. L. Weisenhorn, S. A. C. Gould, R. L. Sinsheimer, H. E. Gaub, G. D. Stucky, C. Zaremba, and P. K. Hansma, *J. Vac. Sci. Technol.* **9**, 1282 (1991).
 - ⁴⁷Arthur W. Adamson, *Physical Chemistry of Surfaces* (Wiley, New York, 1990).
 - ⁴⁸U. Hartmann, *Phys. Rev. B* **43**, 2404 (1991).
 - ⁴⁹Si₃N₄ has a pK ≈ 2; therefore it is negatively charged at neutral pH like mica. Hermann Gaub (private communication).
 - ⁵⁰J. N. Israelachvili and G. Adams, *J. Chem. Soc. Faraday Trans. I* **74**, 975 (1978).
 - ⁵¹Y. L. Chen, C. A. Helm, and J. N. Israelachvili, *J. Phys. Chem.* **95**, 10736 (1991).
 - ⁵²The calculated Debye length of one curve was sometimes very unstable with respect to the number of points used. In this case the Debye length with the highest |r| was chosen as data points for Fig. 7. For a few curves the number of points used was reduced to the regime, where the curve showed clear exponential behavior.